Bachelor's Program in Science and Technology

Experiments on the fracture behavior of steel sheets for hydrogen energy storage application

Ben Nguyen

Aalto University

BACHELOR'S THESIS

Aalto University
BACHELOR'S THESIS 2023

Experiments on the Fracture Behavior of Steel Sheets for Hydrogen Energy Storage Application

Ben Nguyen

Thesis submitted in partial fulfillment of the requirements for the degree of Bachelor of Science in Technology.
Otaniemi, 8 September 2023

Supervisor: professor Luc St-Pierre
Advisor: professor Junhe Lian

Aalto University
School of Science
Bachelor's Program in Science and Technology

Author
Ben Nguyen

Title
Experiments on the Fracture Behavior of Steel Sheets for Hydrogen Energy Storage Application

School School of Engineering

Degree program Bachelor's Program in Science and Technology

Major Computational Engineering **Code** ENG3082

Supervisor professor Luc St-Pierre

Advisor professor Junhe Lian

Level Bachelor's thesis **Date** 8 September 2023 **Pages** 20 **Language** English

Abstract

Hydrogen is suggested to be an alternative fuel, yet hydrogen storage and transportation options are still limited due to safety and economical reasons. However, hydrogen is known for changing material properties in a negative way. Moreover, the material microstructure can change while undergo strain due to forming or other treatments, making the effect of hydrogen unpredictable. As a result, it is necessary to quantify the effect of hydrogen and characterize behavior of metals in different prestrain level.

In this thesis, hydrogen charged properties of 316L and 316L+ stainless steel were determined in monotonic loading conditions and prestrain conditions in order to generate a database for future work and find a predictable pattern for the phenomenon. For prestrain specimens, a prestrain process was conducted in order to achieve the strain level of 0.1 and 0.2. Then the specimens were cathodic hydrogen charged for three days in 50 Celsius degree, then uni-axial tensile tested. The force-displacement and stress-strain curve of these specimens are generated and summarized.

The results provide a better understanding on the effect of hydrogen embrittlement in austenitic stainless steel and the necessary data to characterize 316L and 316L+ reactions to hydrogen diffusion. According to the data, a reduction of ductility was observed across all of the specimens. For the prestrain specimens the ductility loss is relatively unchanged in different strain for 316L, while an increment of ductility loss is seen in 316L+ prestrain samples.

The result suggest a careful consideration of the tested material utilization for hydrogen storage and transportation. The prestrain test purpose that straining from 0 to 0.2 strain level doesn't affect the hydrogen effect, meaning the behaviour of prestrain material with hydrogen embrittlement may be predictable.

Keywords Hydrogen embrittlement, 316L stainless steel, 316L+ stainless steel, Prestrain effect , Nitrogen

urn https://aaltodoc.aalto.fi

Contents

Abstract ii

Contents iii

Symbol and Abbreviation iv

1. Introduction 1

2. Theoretical Background 3

2.1 Hydrogen Diffusion Mechanism of Steel 3

2.1.1 Adsorption of Hydrogen 3

2.1.2 Diffusion of hydrogen and trap theory 4

2.2 Stress triaxiality 5

3. Experimental methods 7

3.1 Testing materials 7

3.2 Uni-axial tension test set-up 7

3.2.1 Prestrain test 8

3.2.2 Fracture test 9

3.3 Hydrogen charge procedure 9

3.3.1 Preparation of specimen and solution 9

3.3.2 Hydrogen charging condition 10

4. Result 12

4.1 Prestrain test 12

4.2 Fracture test 14

5. Discussion 16

6. Conclusion 18

Reference 19

Symbol and Abbreviation

η	Triaxiality
σ	Stress
CH	Center hole
csv	Comma Separated Values
DIC	Digital Image Correlation
FCC	Face Centered Cubic
HE	Hydrogen Embrittlement
NDB	Notched Dog Bone
SDB	Smooth Dog bone
SH(M)	Shear (Moderate)
UTS	Ultimate Tensile Strength

1. Introduction

With the increasing impact of climate change, there is a growing interest of a new energy source that does not produce carbon dioxide. Within the options, such as compress natural gas, many see hydrogen as an ideal choice that can meet such requirement. [1]

Hydrogen is believed by many to be an energy source of the future, even traced back to the 19th century, where it is suggested in Jules Verne's novel The Mysterious Island "I believe that water will one day be used as a fuel, that hydrogen and oxygen, which constitute it, used alone or simultaneously, will provide an inexhaustible source of heat and light of an intensity that coal cannot have."[2]. Hydrogen is reliable as an energy, as it stores as much as 2.8 times energy compare to gasoline[3]. Furthermore, the product of the reaction is water in the form of vapor or liquid. Hence, it is apparent that hydrogen is powerful and sustainable, which is increasingly important for our society to face the current economic and environmental problems.

However, storage and transportation of hydrogen prove to be a difficult problem that cannot be universally resolve[4]. In order for hydrogen to be used as an energy source, the storage must be proven safety and economically available, while fulfil other requirements that are needed in different industries. In order to optimize the use of material for hydrogen storage, it is important to understand the effects of hydrogen on said materials. Because metals go through forming in order to achieve the desired shape, it is also important to consider the effect of strain on the material in combination with hydrogen.

This thesis aim to characterize the failure behaviour of three different geometries (CHD6, SH, NDBR2), as well as the failure behaviour under two prestrain conditions (0.1, 0.2) of 316L and 316L+ stainless steel with and without hydrogen influence.

The remaining of the thesis is divided into 5 sections. In section two, the theoretical understanding related to the research is explained and discussed. Section three describe the experimental equipment and procedures, and section four provide the results from the experiment. Finally, section five and six discuss the results and present a conclusion.

2. Theoretical Background

In this section, the theoretical background supporting the study of hydrogen embrittlement effect on 316L/4404 and 316L+/4420 steel is presented. Hydrogen embrittlement concepts related to the study and basis for the result are discussed.

2.1 Hydrogen Diffusion Mechanism of Steel

2.1.1 Adsorption of Hydrogen

In order for hydrogen to diffuse into steel, mono-atomic hydrogen needed to be adsorb on the interface between the medium and steel. There are three method that for the adsorption of hydrogen: pressurized hydrogen charging, electrolytic hydrogen charging and cathodic hydrogen charging. Pressurized charging initiate hydrogen absorption when hydrogen gas are under pressure and electrolytic charging produce hydrogen through corrosion reaction[5].

The experiment presented in this thesis utilize cathodic charging in order to create hydrogen adsorption. In cathodic hydrogen charging, hydrogen is generated due to an applied potential. Atomic hydrogen formed by the reduction equation of water at the electrode, which has the equation:

$$H_2O\ (aq.) + e^- \longleftrightarrow H\ (ads.) + OH^-.$$

The charging current is the main variable that influence the absorption of hydrogen. Different materials have different potential that maximize the diffusion rate. In addition, the medium also has a difference between using a neutral or acidic solution, as acidic solution can increase the hydrogen density in the specimen due to corrosion. The final factor that affect is the use of "hydrogen poisons", chemical that inhibit the recombination of

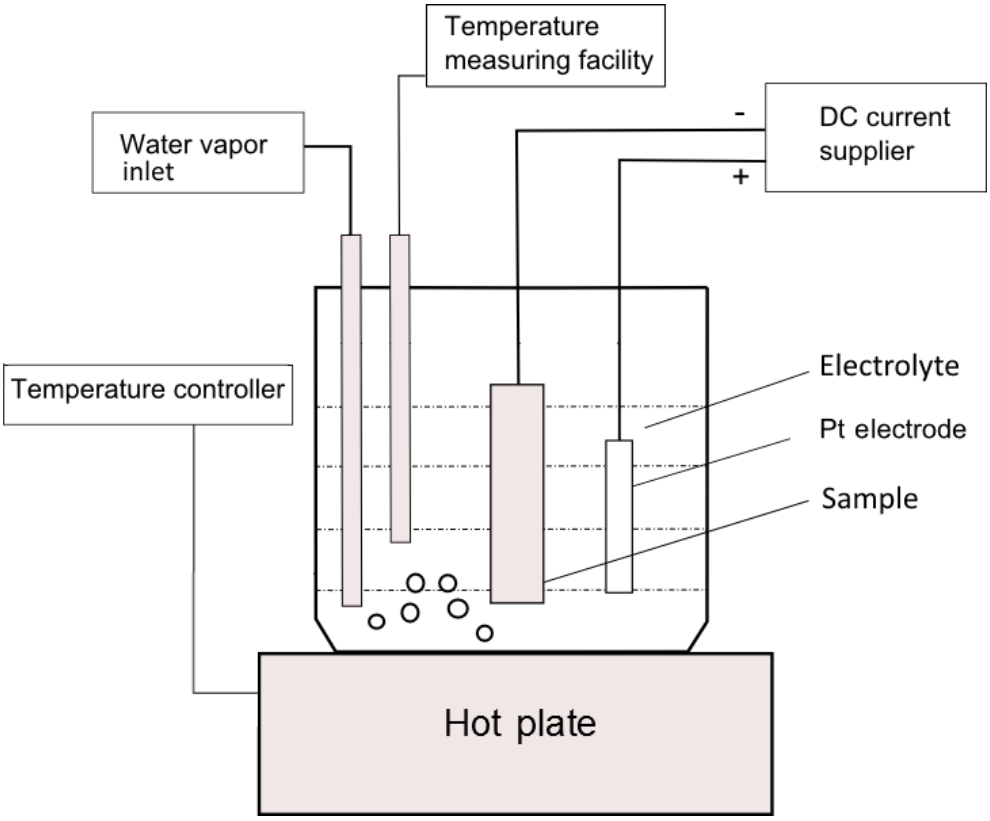

Figure 2.1. Cathodic hydrogen charging set-up[6]

monoatomic hydrogen and hence increase the uptake of hydrogen into the material[5].

Although hydrogen charging process may be different, they lead to the similar effect on hydrogen embrittlement in steel[7].

2.1.2 Diffusion of hydrogen and trap theory

After adsorbing on the surface of steel, monoatomic hydrogen diffuses within the steel lattice. Hydrogen diffusion follow Fick's law:

$$J = -D\frac{\partial \phi}{\partial x}, \tag{2.1}$$

where J is the flux of diffusing particles, D is the diffusivity of hydrogen and C is the hydrogen concentration[8].

However, iron showed a variety in hydrogen diffusion coefficient, notably in room temperature. In order to explain the scatter data in lower temperature, hydrogen trap sites theory was developed.

In trap theory, while hydrogen diffuse rapidly in room temperature, it accumulated vastly in microstructure defect, such as vacancy or grain boundary, which act as trap. Some defect are more attractive, and some are just physical that hydrogen randomly fall into. Some trap are suggested

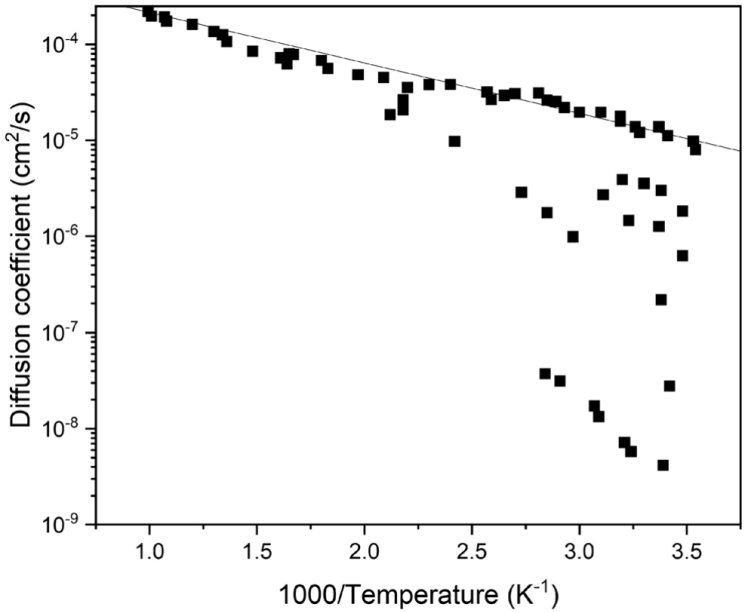

Figure 2.2. Diffusion coefficients of hydrogen in iron [7]

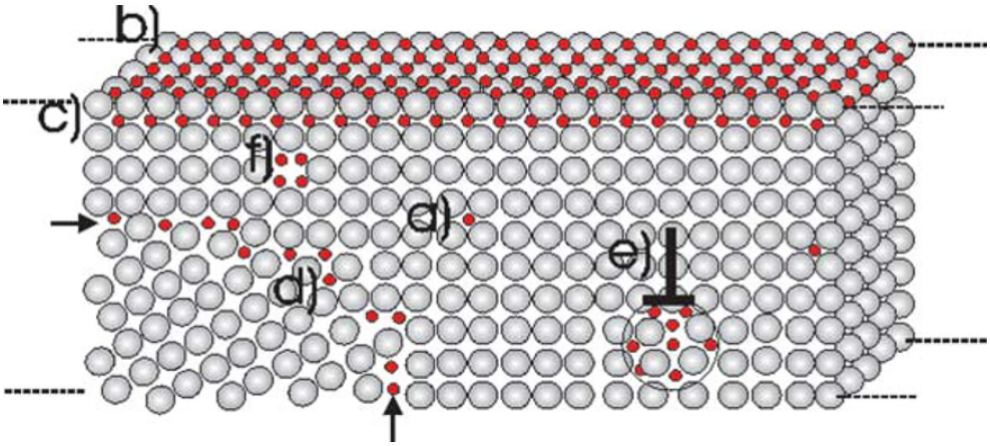

Figure 2.3. Hydrogen amasses at different microstructure defects [9]

to be irreversible, or high trapping energy, meaning that below a certain temperature will not allow hydrogen to escape. As a result, the diffusion coefficient of hydrogen in low temperature is scattered[10].

2.2 Stress triaxiality

In real life application, material are usually under complex and different loading condition, or in other word, different stress state. This is quantified by stress triaxiality parameter, or triaxiality for short, giving the ratio of hydrostatic mean stress to the equivalent von Mises stress. The equation for triaxiality is:

$$\eta = \frac{\sigma_m}{\sigma_{eq}} = \frac{\frac{1}{3}(\sigma_{11}+\sigma_{22}+\sigma_{33})}{\sqrt{\frac{(\sigma_{11}-\sigma_{22})^2+(\sigma_{22}-\sigma_{33})^2+(\sigma_{33}-\sigma_{11})^2+6(\sigma_{12}^2+\sigma_{23}^2+\sigma_{31}^2)}{2}}}. \tag{2.2}$$

Stress triaxiality is commonly related to material strain fracture. In order to generate the dependency, wide range of specimen geometries was designed to investigate the material behavior in different triaxiality. This allow fracture mode prediction and behavior modeling of material in a wide range of stress state[11].

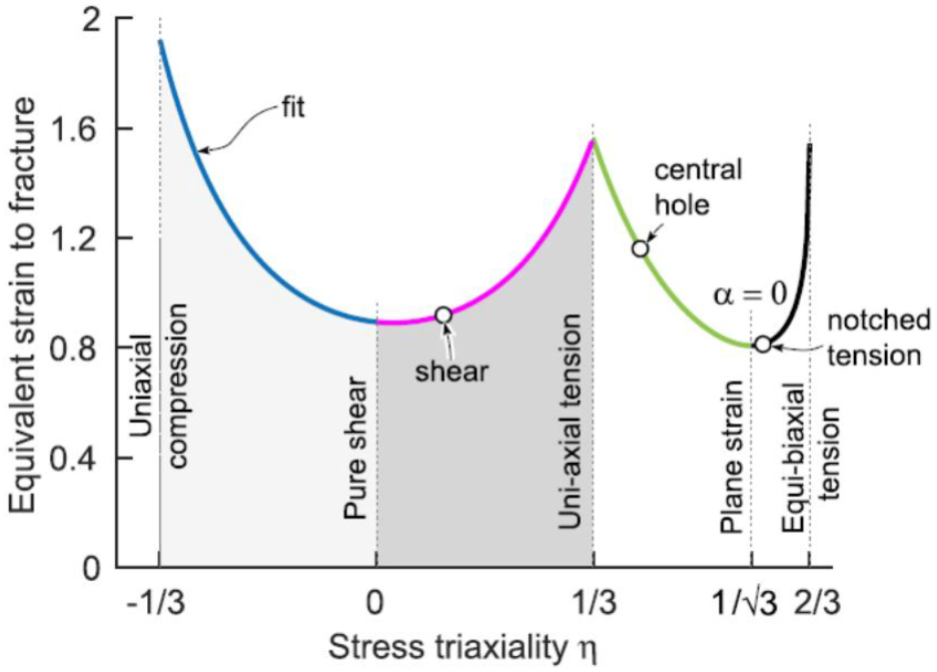

Figure 2.4. The graph show the dependency of stress triaxiality and strain to fracture of steel material [11]

3. Experimental methods

This section provide the information related to the tests conducted for the thesis. Material properties and geometries used for each tests are presented. The methodologies in different part of the test are discussed.

3.1 Testing materials

The test is conducted on two materials: 316L/4404 stainless steel and 316L+/4420 stainless steel. 316L and 316L+ are austenitic (FCC) stainless steels, which have high corrosion resistance and good ductility[12, 13]. The two material have the chemical composition provided in Table 3.1.

	C	Cr	Ni	Mo	N	Other
316L	0.02	17.2	10.1	2.1	-	-
316L+	0.02	20.3	8.6	0.7	0.19	-

Table 3.1. Chemical composition of 316L and 316L+, % by mass [14]

Provided by Outokumpu, the steel sheets are cold rolled and then cut into different geometries for the tensile test. Cold rolling is a process of work hardening process that is often used for stainless steel for enhancing mechanical properties. Metals are pass through rollers at a temperature that is lower than its recrystallization temperature, which change the microstructure, increase the material strength and corrosion resistance. [15]

3.2 Uni-axial tension test set-up

The tensile test is performed by a Zwick/Roell Z030 screw-driven tensile machine. The test is monitored by a computer and track the parameters every second. The export data file from the test provide the information of

the forced and the strain on the specimen. However, because the strain collected is calculated by the distance between two grip, it is highly inaccurate to use this data for analysis.

In order to increase the accuracy and collecting data for further research, a Digital Image Correlation (DIC) system is implemented parallel with the tensile test. DIC is a optical based method used for measuring the displacement or deformation during material testing. The system captures consecutive photo of the material surface during the test, and then analyzed the pictures with computer program.

Prior to the tensile test, the DIC system was calibrated to fit the SDB specimen. The specimen is first cleaned with alcohol and dried to remove any marking paint and ensure a good painting surface. Then, its surface is painted with white paint and leave to completely dry, followed with scatter black paint in order to generate speckle. While the tensile test is in action, the specimen's pictures are taken by two cameras at the rate of one picture every two second.

These image are processed by DIC 3D software to analyze the development of strain at the gauge position. The eyy Lagrange data was able to displayed the evolution of strain during the test, which was recorded in the form of a video. The strain for each geometries was extracted to a csv file in order to correlate with the force data from the tensile machine and then use for analysis.

3.2.1 Prestrain test

For prestrain test, the smooth dog-bone (SDB) geometry was used. Because of its consistent width, the specimens were able to capture the strain both in the longitudinal and transverse direction, allowing a good analysis.

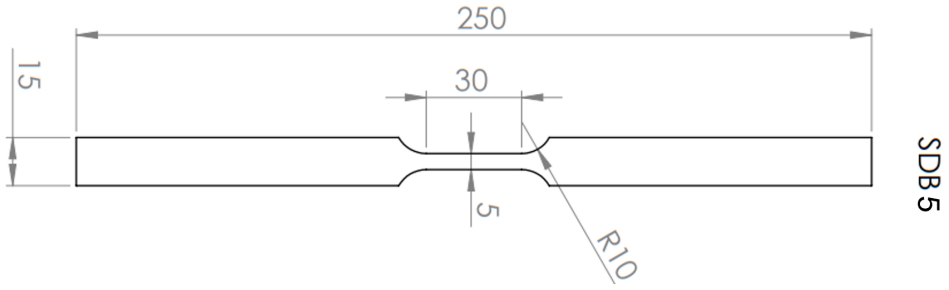

Figure 3.1. The measurement of SDB sample (mm)

The specimen are pulled to 0.1 and 0.2 strain in order to observe the change in ascending strain, with the rate of 0.9mm/min. At the end of the test, the load on the specimen are slowly released with the rate of 1mm/min.

However, due to inaccuracy in measuring the strain by the tensile machine, it is necessary to identify the amount of force that achieved the desired strain and use force as the limit while testing. A data file provided by Aalto University of two material under monotonic loading is sampled to find the corresponding force[16].

	316L	316L+
0.1 strain	3670	4340
0.2 strain	4610	5360

Table 3.2. Amount of force to achieve the strain point (N)

After the specimen are prestrained, for hydrogen embrittlement specimen, the specimens are taken out and charged with hydrogen immediately afterward in order to avoid any aging defect. When the hydrogen charge finished, the specimen are tensile tested with the strain rate of 0.9mm/min.

3.2.2 Fracture test

The fracture test is conducted to investigate the strain to fracture behaviour of different geometries. In this test, three geometries were used: center hole diameter 6 mm (CHD6), notched dog bone radius 2 mm (NDBR2) and shear (SH), covering different triaxiality. The measurement of the geometries are as follow:

Because notches accelerate fracture, the specimen are tested to fracture with the strain rate of 0.45mm/min to capture the necking process for analysis.

3.3 Hydrogen charge procedure

3.3.1 Preparation of specimen and solution

The specimens notch are polished in order to remove the protective coating and ensure a good contact with the charging solution. The sample is first polished in the longitudinal direction with sandpaper grit 800, and then polished in the transverse direction with sand paper grit 1200. Afterward, the sample is cleaned with ethanol in order to remove any substance that can contaminate the charging solution. Finally, the specimen is tape with polytetrafluoroethylene (PTFE) outside of the gauge, so that hydrogen diffusion only happens to the gauge of the specimen, which helps with quantifying the effect of embrittlement. It is important not to touch the

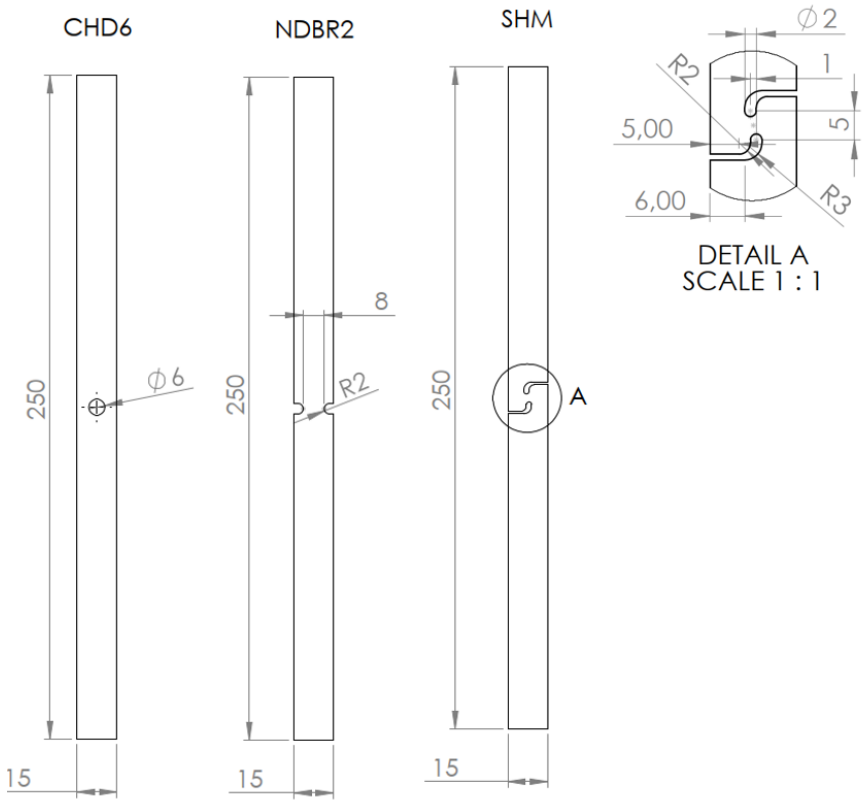

Figure 3.2. The measurement of CH, NDB and SH sample (mm)

clean gauge when taping.

Figure 3.3. Image of a prepared sample

The charging solution used for the experiment is 1N H_2SO_4 with added Thiourea as the "hydrogen poison" (20 mg/l). One charging session use 1.25 litter of charging solution. To create the solution, 1216 ml of distilled water, 34 ml of 98% H_2SO_4 solution and 25 mg of Thiourea are mixed inside a flask.

3.3.2 Hydrogen charging condition

Due to the corrosive resistant nature of the material, the charging condition is designed in order to stimulate the diffusion of hydrogen. The specimen is charged inside a three-electrode electrochemical cell with a curved Luggin

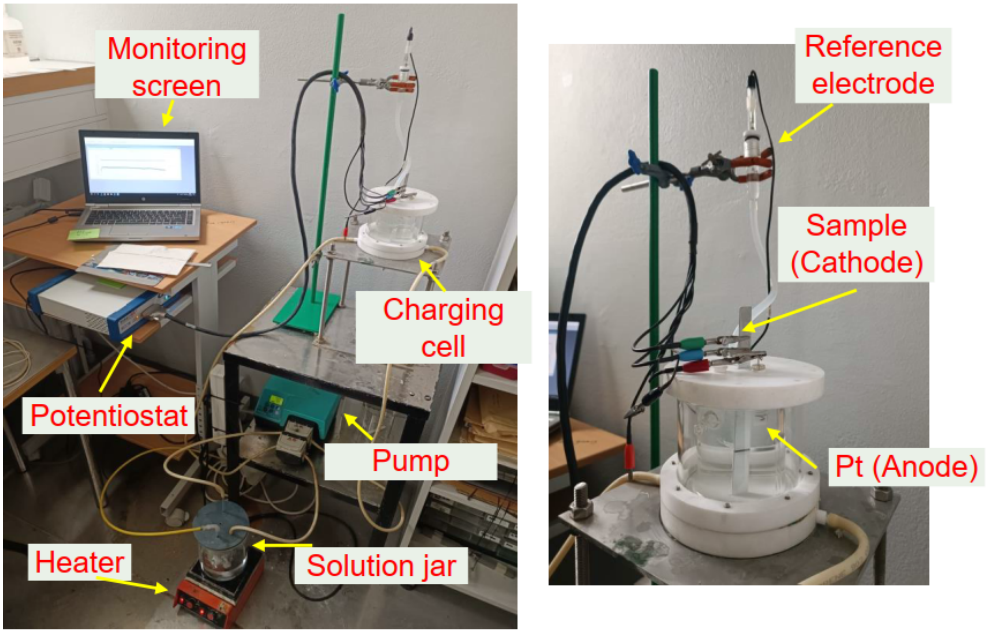

Figure 3.4. Hydrogen charging set-up in Aalto University [16]

salt bridge filled with K_2SO_4 reference electrode and Pt counter electrode, monitored by a Gamry potentiostat during the charging session. In order to keep the solution concentration consistent, the cell is connected with a pump and a conditioning container that contain the excess solution. The condition is set using a magnetic stirrer, which was adjusted so that 50 Celsius degree is recorded in the charging cell. The solution cycle through as the pump is set to 70 rotation per minute.

The clean specimen is put inside the hydrogen charge cell such that the gauge is put close to the cell reference electrode. In order for the hydrogen to charge correctly, the membrane of the electrode need to be ensured that there is no clogging as a disconnection from the electrode will corrode and damage the specimen, making the amount of embrittlement unpredictable.

The hydrogen cathodic charging is activated using the monitoring computer. The system is left to charge in 72 hours and check frequently. When the charging time is reached, the electrolysis stop and the solution is pumped out and discard. The specimen is taken out and cleaned with cold water and ethanol, and then used to do the tensile test immediately in order to reduce the loss of hydrogen to the environment.

4. Result

For every specimens, two tests was conducted with and without hydrogen charging in order to ensure repeatability. However, due to the constrain of time, only one NDBR2 specimen was tested. As the result, 39 tests have been conducted for the project.

4.1 Prestrain test

For the prestrain specimens, the engineering and true stress-strain curve is presented in figure 4.1, 4.2, 4.3, 4.4. The mechanical properties recorded from the tests are summarized in Table 4.1.

The result shows a clear reduction in ductility of both material in hydrogen charged specimens, while other parameter have minimal to no changes. It can be seen from the graph and the table that there is a slight increase in ultimate tensile strength of the two steel.

In the 0.1 strain category, the hydrogen charged 316L specimens experience a 7.83% loss and 316L+ experience a 7.22% loss in deformation capacity. Moreover, in 0.2 strain, the reduction in ductility due to HE have an increase to 8.86% in 316L specimens and 8.44% in 316L+ specimens. However, it is worth mentioning that the fracture strain in HE samples have a difference of approximately 0.3% and because the value are small, the error or difference in samples can be magnified.

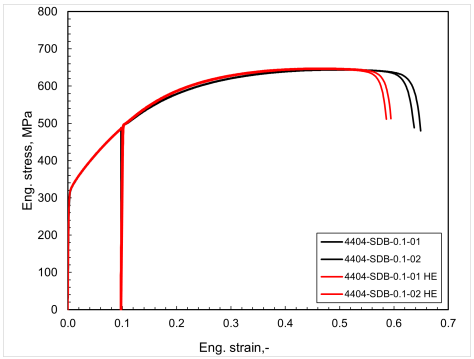

(a) 316L/4404

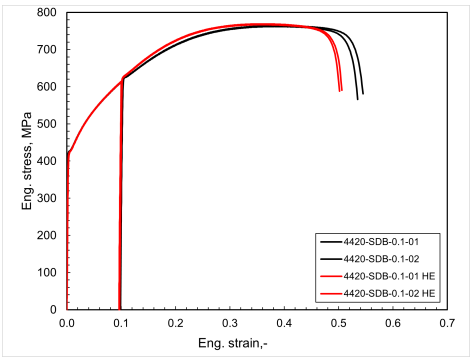

(b) 316L+/4420

Figure 4.1. The Engineering Stress-Strain Curve at 0.1 strain

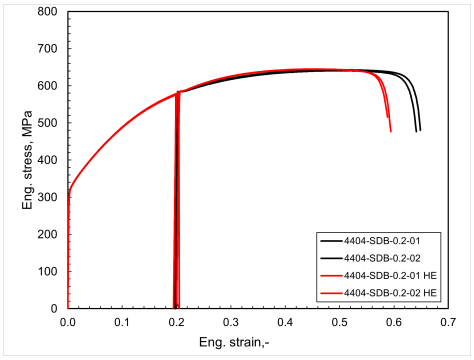

(a) 316L/4404

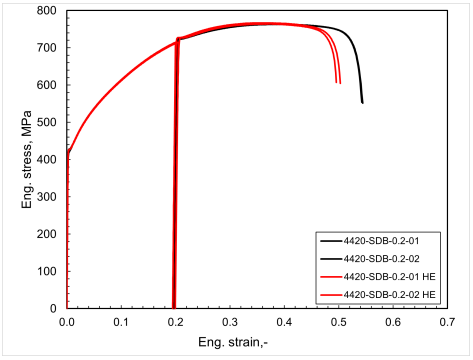

(b) 316L+/4420

Figure 4.2. The Engineering Stress-Strain Curve at 0.2 strain

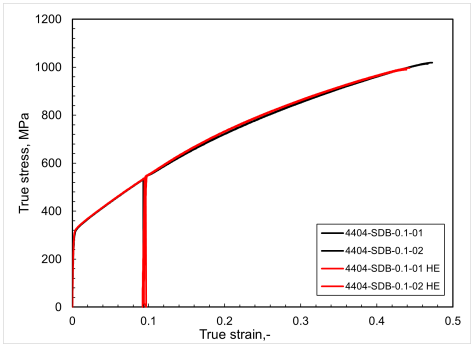

(a) 316L/4404

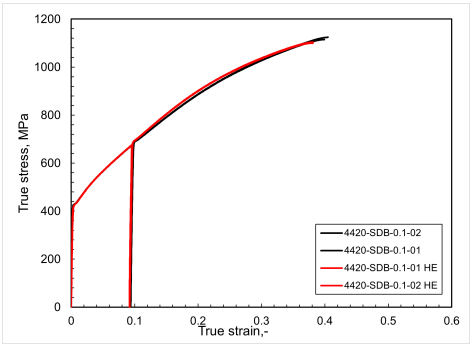

(b) 316L+/4420

Figure 4.3. The True Stress-Strain Curve at 0.1 strain

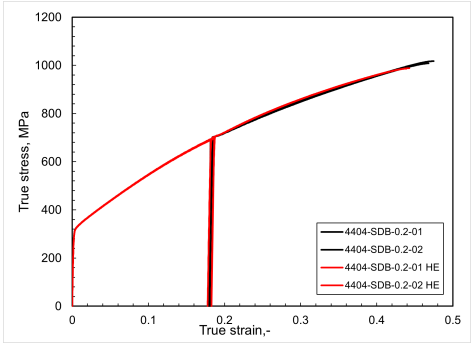

(a) 316L/4404

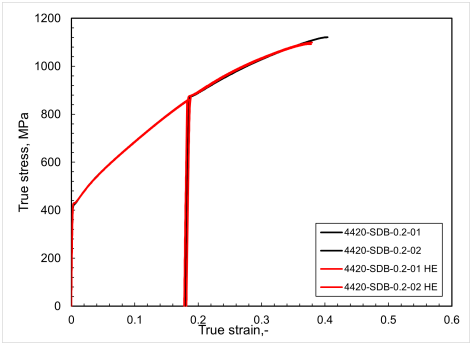

(b) 316L+/4420

Figure 4.4. The True Stress-Strain Curve at 0.2 strain

		0.1 strain	0.2 strain
316L/4404	Fracture strain	0.645	0.654
	Fracture strain (HE)	0.594	0.596
	Loss	7.83%	8.86%
	UTS	644	642
	UTS (HE)	645	644
		0.1 strain	0.2 strain
316L+/4420	Fracture strain	0.54	0.545
	Fracture strain (HE)	0.501	0.499
	Loss	7.22%	8.44%
	UTS	763	763
	UTS (HE)	766	766

Table 4.1. Prestrain test engineering stress-strain summary

4.2 Fracture test

The data for CHD6 and NDBR2 are presented in Table 4.2. Although CHD6 have a higher loss in ductility to HE than NDBR2, the elongations from CHD6 specimens are always higher than its NDBR2 counterpart.

For the shear test, the specimens used was unable to provide the data for shear fracture mode. During the test, the specimen first necked at the center of the gauge, signaling a shearing failure. However, the specimen did not fracture then but went on and neck in a different position, on the upper left or lower right of the specimen gauge and fractured, showing more of a tensile failure mode than shear.

		316L	316L+
CHD6	Elongation (mm)	4.15	3.74
	Elongation HE (mm)	3.55	3.3
	Loss	14.4%	11.8%
		316L	316L+
NDBR2	Elongation (mm)	3.83	3.49
	Elongation HE (mm)	3.495	3.26
	Loss	8.74%	6.6%

Table 4.2. Fracture test on CHD6 and NDBR2 summary

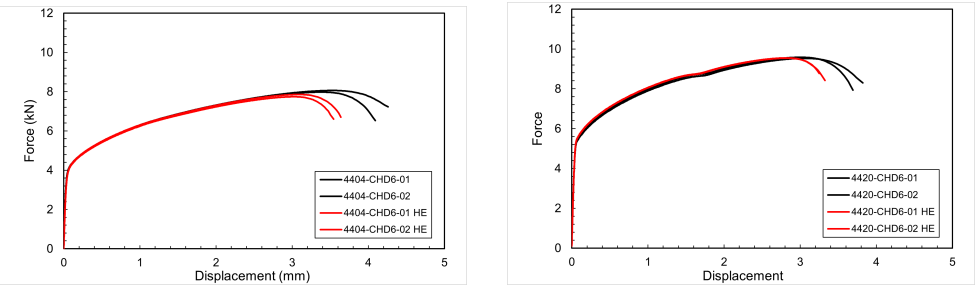

(a) 316L/4404 **(b)** 316L+/4420

Figure 4.5. Force-Displacement Graph of CHD6

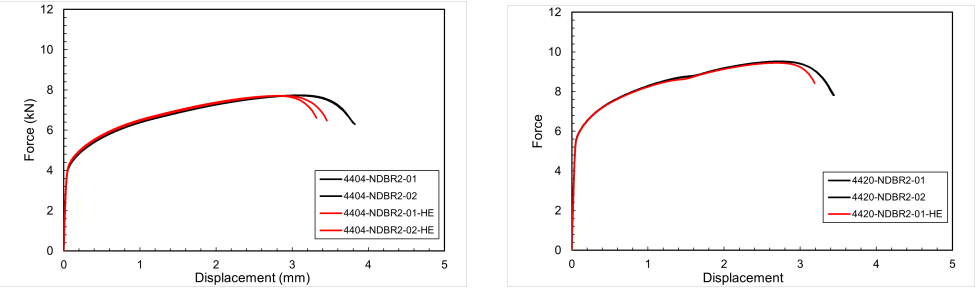

(a) 316L/4404 **(b)** 316L+/4420

Figure 4.6. Force-Displacement Graph of NDBR2

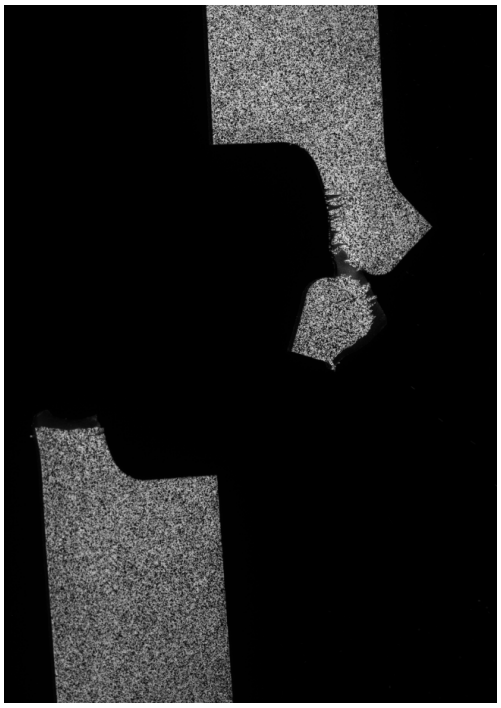

Figure 4.7. Shear specimen failure not on shear mode

5. Discussion

The result have shown the effect of hydrogen embrittlement on 316L and 316L+, demonstrating different reduction in ductility. It is consistent throughout the test that 316L+ is more resistant to HE compare to 316L, as the loss of ductility in each test of 316L+ are lower. This result suggests the introduction of nitrogen in the steel composition may increase the resistance to HE. Through increasing the stability of austenite, nitrogen can decrease the hydrogen-induced loss of the steel[17].

The monotonic loading data for 316L and 316L+ was provided by Aalto University for analysis[16]. The comparison in different strain rate is shown in Figure 5.1 and 5.2, summarised in Table 5.1.

In the prestrain specimens, the data from 316L specimens suggest a miniscule positive correlation of hydrogen embrittlement effect with the strain level. As the specimens are strained, new voids are generated which may act as new trap sites and increase the HE effect[18, 19]. However, the change in fracture strain is minimal to none compare to the change of strain level. The reason for this may be that as the specimen unload, its microstructure reorganizes itself and partially fills the new void and reduce their trapping effects. However, there is a difference in the data from 316L+ specimens. A reduction in ductility is observed in the prestrain specimens compare to the monotonic loading specimens. The microstructure of 316L+ may have been altered due to straining, reducing the strengthening effect of nitrogen and making the steel more vulnerable to hydrogen embrittlement.

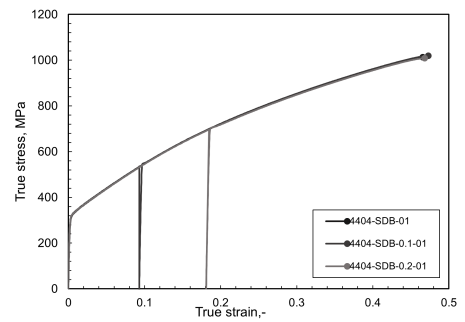

(a) Without hydrogen charging **(b)** With hydrogen charging

Figure 5.1. True stress-strain curve of 316L/4404

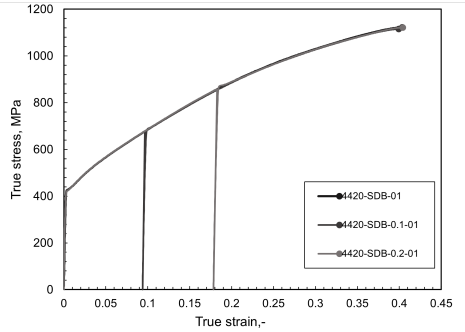

(a) Without hydrogen charging **(b)** With hydrogen charging

Figure 5.2. True stress-strain curve of 316L+/4420

		Normal	0.1 strain	0.2 strain
316L/4404	Fracture strain	0.465	0.4795	0.4752
	Fracture strain (HE)	0.445	0.4429	0.4425
	Loss	4.3%	7.63%	6.92%
316L+/4420		Normal	0.1 strain	0.2 strain
	Fracture strain	0.402	0.41	0.41
	Fracture strain (HE)	0.394	0.39	0.388
	Loss	1.99%	4.87%	5.36%

Table 5.1. Prestrain test true stress-strain comparison summary

6. Conclusion

The conclusions of the research on characterizing the effect of hydrogen embrittlement on 316L and 316L+ stainless steel is listed bellow.

- Hydrogen embrittlement effects on mechanical properties of steel is mainly ductility, with 14.4% loss in the most severe case. There is also a slight increase in UTS in engineering stress-strain curve of most case observed.

- Nitrogen alloying in steel increase austenite stability and reduce the effect of hydrogen embrittlement. 316L+ have a higher corrosive resistivity and more resistant to HE compare to 316L.

- 316L/4404 and 316L+/4420 have a strong resistance to shear failure, with and without HE effect.

- Prestrained specimen (up to strain level 0.2) shown a minimal effect on hydrogen embrittlement. However, straining reduce nitrogen effect and as a result reduce the hydrogen embrittlement resistivity in materials that contain nitrogen.

Reference

[1] A. Dhabi., "Hydrogen from renewable power: Technology outlook for the energy transition, international renewable energy agency," tech. rep., IRENA, 2018.

[2] J. Verne, *The Mysterious Island*. Wordsworth Editions Ltd., 2010.

[3] A. F. D. Center, "Hydrogen basics." https://afdc.energy.gov/fuels/hydrogen_basics.html.

[4] D. Mori and K. Hirose, "Recent challenges of hydrogen storage technologies for fuel cell vehicles," *International Journal of Hydrogen Energy*, vol. 34, no. 10, pp. 4569–4574, 2009. 2nd World Hydrogen Technologies Convention.

[5] M. Truschner *et al.*, "The basics of hydrogen uptake in iron and steel," *Berg Huettenmaenn Monatsh*, 2021.

[6] C. Bjerkén, M. Fisk, and N. Ehrlin, "Cathodic hydrogen charging of inconel 718," *AIMS Materials Science*, vol. 3, pp. 1350–1364, 01 2016.

[7] M. L. Martin, M. J. Connolly, F. W. DelRio, and A. J. Slifka, "Hydrogen embrittlement in ferritic steels," *Applied Physics Reviews*, vol. 7, p. 041301, 10 2020.

[8] H. Wipf, "Solubility and diffusion of hydrogen in pure metals and alloys," vol. 2001, p. 43, jan 2001.

[9] A. Pundt and R. Kirchheim, "Hydrogen in metals: Microstructural aspects," *Annual Review of Materials Research*, vol. 36, no. 1, pp. 555–608, 2006.

[10] J.-Y. Lee and S. Lee, "Hydrogen trapping phenomena in metals with b.c.c. and f.c.c. crystals structures by the desorption thermal analysis technique," *Surface and Coatings Technology*, vol. 28, no. 3, pp. 301–314, 1986.

[11] M. Kõrgesaar, "The effect of low stress triaxialities and deformation paths on ductile fracture simulations of large shell structures," *Marine Structures*, vol. 63, pp. 45–64, 2019.

[12] Outokumpu, "Supra 316L/4404." https://secure.outokumpu.com/steelfinder/Properties/GradeDetail.aspx?OTKBrandNameID=00602&Category=Supra.

[13] Outokumpu, "Supra 316plus." https://secure.outokumpu.com/steelfinder/Properties/GradeDetail.aspx?OTKBrandNameID=00607&Category=Supra.

[14] Outokumpu, "Compare product." https://www.outokumpu.com/fi-fi/compare-products?items={88901B28-3DD3-4389-AA7D-CA179FA02ADC}|{246C3939-5F59-4489-804F-A3B402593CF6}&colors=306084|306084&ret=/.

[15] Ulbrich., "What is cold rolled stainless steel and other metals?." https://www.ulbrich.com/blog/what-is-cold-rolling-stainless-steel-and-other-metals/.

[16] M. Argandoña, "Hydrogen embrittlement characterisation for fcc steels for h2 storage and transport," 2022-2023.

[17] K.-S. Kim, J.-H. Kang, and S.-J. Kim, "Nitrogen effect on hydrogen diffusivity and hydrogen embrittlement behavior in austenitic stainless steels," *Scripta Materialia*, vol. 184, pp. 70–73, 2020.

[18] P. J. Noell, J. D. Carroll, and B. L. Boyce, "The mechanisms of ductile rupture," *Acta Materialia*, vol. 161, pp. 83–98, 2018.

[19] A. Pineau, A. Benzerga, and T. Pardoen, "Failure of metals i: Brittle and ductile fracture," *Acta Materialia*, vol. 107, pp. 424–483, 2016.